

Annealing of radiation induced oxygen deficient point defects in amorphous silicon dioxide:  
evidence for a distribution of the reaction activation energies

This article has been downloaded from IOPscience. Please scroll down to see the full text article.

2008 J. Phys.: Condens. Matter 20 385215

(<http://iopscience.iop.org/0953-8984/20/38/385215>)

View [the table of contents for this issue](#), or go to the [journal homepage](#) for more

Download details:

IP Address: 129.252.86.83

The article was downloaded on 29/05/2010 at 15:08

Please note that [terms and conditions apply](#).

# Annealing of radiation induced oxygen deficient point defects in amorphous silicon dioxide: evidence for a distribution of the reaction activation energies

L Nuccio<sup>1</sup>, S Agnello and R Boscaino

Dipartimento di Scienze Fisiche ed Astronomiche, University of Palermo, Via Archirafi 36, I-90123 Palermo, Italy

E-mail: [laura.nuccio@fisica.unipa.it](mailto:laura.nuccio@fisica.unipa.it)

Received 18 April 2008, in final form 15 July 2008

Published 27 August 2008

Online at [stacks.iop.org/JPhysCM/20/385215](http://stacks.iop.org/JPhysCM/20/385215)

## Abstract

The selective annealing of point defects with different activation energies is studied, by performing sequences of thermal treatments on gamma irradiated silica samples in the temperature range 300–450 °C. Our experiments show that the dependence on time of the concentration of two irradiation induced point defects in silica, named ODC(II) (standing for oxygen deficient centre II) and the  $E'_\gamma$  centre, at a given temperature depends on the thermal history of the sample for both of the centres studied; moreover in the long time limit this concentration reaches an asymptotic value that depends on the treatment temperature alone.

These results suggest the existence of a distribution of the activation energies of the reaction process responsible for the annealing of the defects investigated, intimately related to the intrinsic disorder of the amorphous lattice. Furthermore, our data show that the thermal treatment can modify this distribution of activation energies and as a consequence the thermal properties of the centre itself.

## 1. Introduction

Amorphous silicon dioxide (a-SiO<sub>2</sub>), or silica, is usually considered a model system for the study of the properties of amorphous materials. This fact, together with the wide use of this material in the production of electronic and optical devices, has been holding the interest in a-SiO<sub>2</sub> for many years. Particular attention has always been devoted to the study of the properties of point defects in silica, due to the fact that their presence is often associated with optical absorption (OA) and photoluminescence (PL) bands that can compromise the characteristic features of the material.

An always increasing attention is nowadays paid to the effect of thermal treatments on point defects. Indeed this kind of procedure can influence the properties of the material and as a consequence it is widely employed in the production of devices, or it can be used to anneal point defects induced by

irradiation, and in some cases can also be a way to obtain information on defects properties [1, 2].

The annealing of point defects following a thermal treatment of the sample can be attributed to different microscopic processes and, even if the first mechanism responsible for these effects was thought to be the recombination of radiolytic electron hole pairs, today it is commonly believed that the main process giving rise to such effects is the reaction of the defects with molecules diffusing through the matrix, as hydrogen, oxygen or water [1, 3–8]. This kind of process is generally described as the result of the concurrence of two distinct phenomena, the diffusion of the molecule and its reaction with the defect. So the observed rate for the annealing process of a point defect is determined by the characteristic timescales of both these phenomena, even if in some cases one of them can be predominating.

A class of widely studied point defects is that of oxygen deficiency related centres, since they give rise to optical absorption and photoluminescence bands in the ultraviolet

<sup>1</sup> Author to whom any correspondence should be addressed.

spectral range, to electron paramagnetic resonance (EPR) signals, and they can also play the role of precursors for other point defects [9, 10].

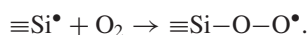
In this paper our attention is focused on two of them, named the  $E'_\gamma$  centre and oxygen deficient centre II (ODC(II)).

The  $E'_\gamma$  centre is a paramagnetic point defect always present in irradiated silica, whose structural model is a threefold coordinated silicon atom having an unpaired electron in one of its hybrid  $sp^3$  orbitals  $\equiv\text{Si}\bullet$ , where  $\equiv$  represents three bonds with oxygen atoms and  $\bullet$  is an unpaired electron. The presence of the unpaired electron gives rise to a characteristic EPR signal around  $g \approx 2.0006$ ; the  $E'_\gamma$  centre is also responsible for an OA band at 5.8 eV with FWHM 0.7 eV [10].

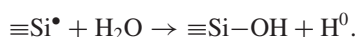
The ODC(II) is a diamagnetic defect whose main spectral features are an OA band centred at  $\sim 5.0$  eV, usually named  $B_{2\alpha}$  band, inside which two PL emission bands centred at  $\sim 4.4$  eV ( $\alpha_1$  band) and at  $\sim 2.7$  eV ( $\gamma$  band) can be excited [10]. Its microscopic structure, differently from that of the  $E'_\gamma$  centre, is still subject of debate. According to some authors the defect responsible for the above described optical activity is an unrelaxed oxygen vacancy:  $\equiv\text{Si}-\text{Si}\equiv$  [11–14]. Nevertheless, many other authors support a twofold coordinated silicon model for the ODC(II),  $\equiv\text{Si}^{\bullet\bullet}$ , that is nowadays widely accepted [9, 15–17].

The effects of heat treatments on these defects have been studied and some microscopic models of reaction have been put forward. As reported in literature the microscopic mechanism of the annealing of a given defect depends on the temperature and on the type of silica [1, 12]. In particular, the annealing of  $E'_\gamma$  centre observed at temperatures higher than about  $-70^\circ\text{C}$  is known to be due to reactions with molecular hydrogen [14, 18–21]. This process has been attributed to the hydrogen diffusion, and has been widely studied, also due to the ubiquitous presence of this impurity in silica [12, 18, 22]. It has been established that the activation energy for  $\text{H}_2$  diffusion in silica is distributed, as a consequence of the amorphous nature of the material [12, 22–24].

A few studies at higher temperatures have also been carried out, and the annealing of the  $E'_\gamma$  centre has been attributed to reactions with other small molecules diffusing through the matrix [1, 12]. In low OH concentration silica the annealing of the  $E'_\gamma$  centre at temperature higher than  $\sim 150^\circ\text{C}$  has been attributed to the reaction with oxygen [25]

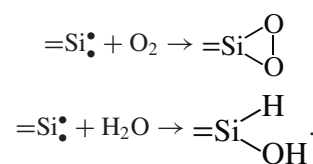


The annealing of the  $E'_\gamma$  centre observed in high OH silica at temperatures higher than  $\sim 300^\circ\text{C}$  has instead been attributed to the reaction with water [1]



Based on the observation of a strong similarity between the isochronal anneal curves of the two defects, the annealing of ODC(II) has been tentatively ascribed to reactions with the same molecules involved in the  $E'_\gamma$  centre annealing in each of the different temperature ranges, according to the

reactions [4, 26–28]



Notwithstanding the increasing number of works about the diffusion of small molecules, different from hydrogen, in silica and their interaction with point defects at temperatures higher than  $100^\circ\text{C}$  [3, 8, 29], the effects of the disorder of the glass matrix on these diffusion–reaction processes have not been studied yet. Data on this subject are only available for processes related to hydrogen, at temperatures equal or lower than room temperature, for which distributions of the activation energy of diffusion have been assumed in the fitting procedures. However no distribution of the activation energy for reaction has been introduced. Data at higher temperatures, at which reactions of point defects with different molecules occurs, and evidences of the influence of the disorder on the activation energies for reaction are not available.

In the present paper we give a direct experimental evidence that the activation energies of the reaction processes responsible for the annealing of point defects in amorphous silicon dioxide at higher temperatures are distributed, due to the disorder characteristic of the glass matrix.

## 2. Experimental details

### 2.1. Measurements

Electron paramagnetic resonance (EPR) has been used to detect the  $E'_\gamma$  centre, whereas photoluminescence (PL) and optical absorption (OA) have been employed to reveal the diamagnetic ODC(II) centre. Raman spectroscopy has been also used to detect interstitial oxygen molecules. EPR measurements have been carried out using a Bruker EMX spectrometer working at 9.8 GHz (X band). The  $E'_\gamma$  centre signal has been revealed with a microwave power  $P = 0.8 \mu\text{W}$  and a modulation field with peak-to-peak amplitude  $B_m = 0.01$  mT and frequency  $f_m = 100$  kHz. These EPR measurement conditions have been verified not to distort the EPR lineshape and not to induce microwave saturation effects. Defect concentration has been estimated by comparing the double integral of the EPR signal of the sample under examination with that of  $E'_\gamma$  centres in a silica sample whose defect concentration has been determined by spin-echo experiments [30]. We have estimated an absolute accuracy of 20% in this procedure; the relative concentrations are affected by a 5% uncertainty. A typical EPR spectrum of  $E'_\gamma$  centre, as detected in one of the sample studied in this paper, is shown in figure 1.

Steady-state PL emission in the range 2.5–5.0 eV, excited at 5 eV, has been measured using a Jasco FP-6500 instrument, mounting a xenon lamp of 150 W, with a bandwidth of 5 nm for excitation and 3 nm for emission. We have adopted the so-called  $45^\circ$ -backscattering-geometry, in which the surface of the sample is placed at  $45^\circ$  with respect to the excitation beam and the PL light is collected in the direction opposite to the

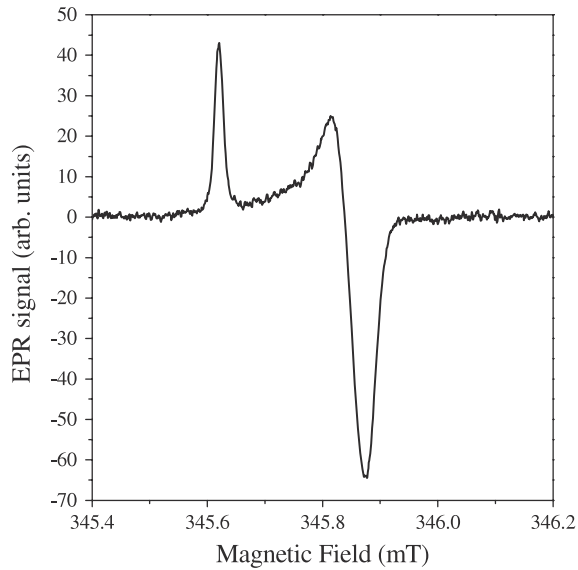


**Figure 1.** EPR spectrum detected in the I301/A sample.

reflected beam. A typical PL spectrum of the ODC(II) centre, as detected in one of the sample studied in this paper, is shown in figure 2; in the inset of the same figure the PLE spectrum relative to the emission at 4.4 eV is shown.

OA measurements in the range 3.0–6.2 eV have been performed using a Jasco V-560 spectrophotometer with a bandwidth of 2 nm.

PL amplitude values have been corrected to take into account differences in the optical absorption of the sample and differences in sample thickness. As the maximum OA intensity at 5.0 eV is less than  $1.2 \text{ cm}^{-1}$  in all the samples examined, and the thickness of the samples is 1 mm, the PL intensity is proportional to the absorption coefficient  $\alpha$ , and so to the concentration of the defects. As a consequence it has been possible to estimate the concentration of the ODC(II) using the Smakula's equation [2] and a reference sample in which the  $B_{2\alpha}$  band was isolated. On the basis of approximations related to Smakula's equation we have estimated an absolute accuracy of 30% in this procedure [2]. The relative concentrations are affected by a 10% uncertainty.

Raman spectra have been measured with Nd-YAG laser excitation ( $\lambda = 1064 \text{ nm}$ ) using a Bruker RamII Fourier-transform spectrometer. The spectral resolution of these measurements was  $5 \text{ cm}^{-1}$ . It has been shown that an infrared PL band at 1272.2 nm excited at 1064 nm (Nd-YAG laser), associated to the forbidden transition from the first electronic excited state ( $a^1\Delta_g$ ) to the ( $X^3\Sigma_g^-$ ) ground state of the interstitial oxygen molecule, superimposes to the Raman spectrum of samples having an oxygen concentration higher than  $5 \times 10^{16} \text{ molecules cm}^{-3}$  [31].

All the measurements have been carried out at room temperature.

## 2.2. Materials and treatments

Two different sets of experiments are presented hereafter.

In the former, three samples of the same natural dry material [32], Infrasil 301 [33] (referred to as I301/A, I301/B

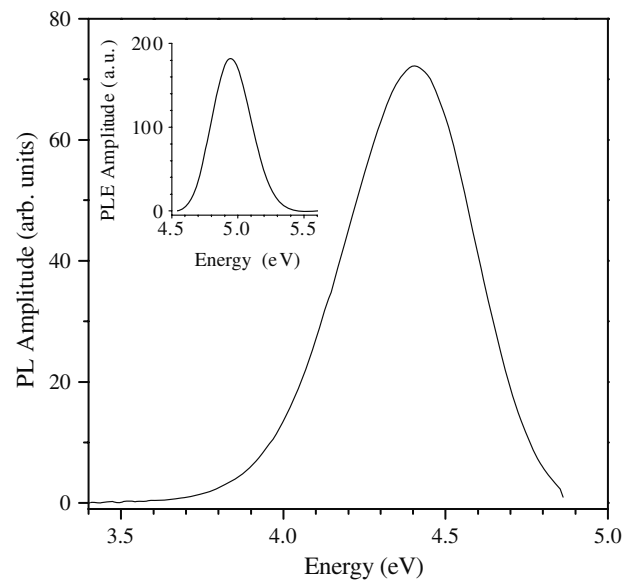


**Figure 2.** PL emission spectrum excited at 5.0 eV as detected in the I301/A sample. In the inset the corresponding PLE spectrum as detected at the emission energy of 4.4 eV is shown.

and I301/C in the following), have been used. Preliminary to every experiment described in the following, they have been  $\beta$  irradiated at room temperature in a linear accelerator (electron energy 3 MeV, dose rate  $\sim 430 \text{ kGy h}^{-1}$ ), up to a total dose of 2000 kGy, so that the concentrations of a given defect before the thermal treatments were approximately the same in all the samples. In particular, the  $E'_\gamma$  centre concentration has been estimated to be about  $4.5 \times 10^{17} \text{ centres cm}^{-3}$  in all the samples and that of ODC(II) varied between  $3.5 \times 10^{15}$  and  $5.7 \times 10^{15} \text{ centres cm}^{-3}$ .

In the second experiment two samples of the natural dry material Silica EQ906 [34], named Q906/A and Q906/B, have been  $\gamma$  irradiated ( $^{60}\text{Co}$  source, dose rate of  $\sim 20 \text{ kGy h}^{-1}$ ) at two different doses: 2500 kGy and 10000 kGy, respectively, so that the ODC(II) concentration in the second sample ( $2.4 \times 10^{15} \text{ centres cm}^{-3}$ ) was higher than in the first one ( $1 \times 10^{15} \text{ centres cm}^{-3}$ ). The  $E'_\gamma$  concentration was instead about  $1 \times 10^{17} \text{ centres cm}^{-3}$  in both samples.

The sizes of all the samples were  $5 \times 5 \times 1 \text{ mm}^3$ , and they were cut from slabs of each material with size  $50 \times 5 \times 1 \text{ mm}^3$ , having the widest surfaces optically polished.

The samples have been subjected to isothermal heat treatments at 200, 300 and 450 °C in an electric furnace whose temperature has been set by means of a digital controller. The target temperature can be set with an accuracy of  $\pm 3 \text{ }^\circ\text{C}$ . As described in the following, isothermal treatments, i.e. series of heat treatments at a fixed temperature and whose duration progressively increases, have been carried out at several temperatures. The duration of the individual treatment varied from 60 s up to  $\sim 10^5 \text{ s}$ . At each treatment the sample is inserted into the oven, that has previously reached the target temperature, and at the end it is extracted from the oven and brought back to room temperature in air to carry out the measurements. This heating and cooling conditions have been chosen to minimize the time that the sample spends

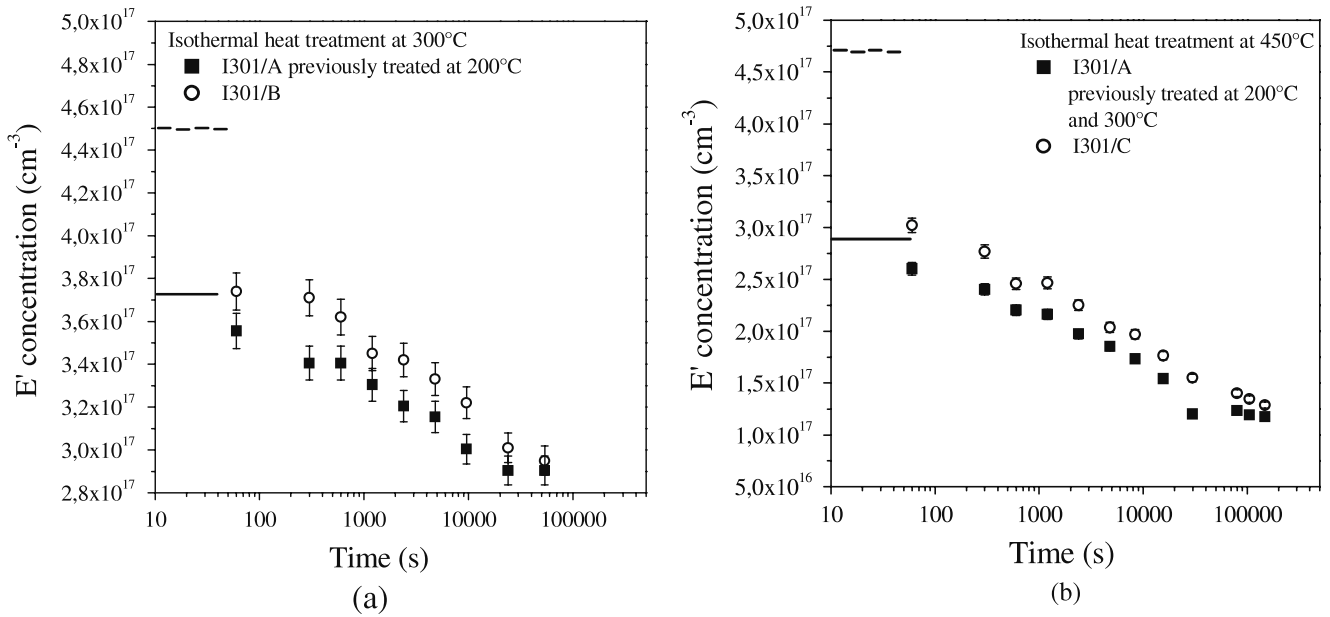


**Figure 3.** (a) Concentration of  $E'_\gamma$  centres as a function of the treatment time at 300 °C, as detected in the samples I301/A, previously treated at 200 °C (filled symbols), and I301/B, not previously treated (open symbols). Solid and dashed lines represent the concentration of  $E'_\gamma$  centres respectively in the samples I301/A and I301/B before the beginning of the treatment at 300 °C. (b) Concentration of  $E'_\gamma$  centres as a function of the treatment time at 450 °C, as detected in the samples I301/A, previously treated at 200 °C and 300 °C (filled symbols), and I301/C, not previously treated (open symbols). Solid and dashed lines represent the concentration of  $E'_\gamma$  centres respectively in the samples I301/A and I301/C before the beginning of the treatment at 450 °C.

**Table 1.** Variations of the concentration of  $E'_\gamma$  centres observed in the experiment on the I301 samples at different temperatures.

Sample	$\Delta[E']$ at 200 °C	$\Delta[E']$ at 300 °C	$\Delta[E']$ at 450 °C
I301/A	$8 \times 10^{16}$ centres $\text{cm}^{-3}$	$8 \times 10^{16}$ centres $\text{cm}^{-3}$	$1.9 \times 10^{17}$ centres $\text{cm}^{-3}$
I301/B		$1.5 \times 10^{17}$ centres $\text{cm}^{-3}$	
I301/C			$3.5 \times 10^{17}$ centres $\text{cm}^{-3}$

at temperatures different from the target temperature of the treatment.

### 3. Results

We have found that the spectral shape of the PL band related to ODC(II) is not affected throughout the overall thermal treatments in the experiments shown in the following, whereas the  $E'_\gamma$  centre features a slight variation of its lineshape, as previously reported [12, 35]. So, the main effect of the thermal treatments is the reduction of the concentration of the defects.

#### 3.1. Treatments on Infrasil 301

In this experiment the three samples of the material I301 described in section 2.2 have been used. The isothermal anneal curves at a given temperature, that represent the defect concentration as a function of the treatment time, have been compared for samples subjected to different sequences of thermal treatments.

The sample I301/A has been thermally treated at 200 °C for 100 000 s. After this preliminary treatment this sample and the I301/B have been subjected to the same isothermal treatment at 300 °C. In figure 3(a) the isothermal anneal curves at 300 °C for the  $E'_\gamma$  centres in the samples I301/A

and I301/B are shown. The lines indicate the concentration of  $E'_\gamma$  centres before the beginning of the thermal treatment at 300 °C in the samples I301/A (solid line) and I301/B (dashed line). The overall duration of the thermal treatment has been chosen in such a way that the annealing processes had reached a stationary state.

Figure 3(b) shows the analogous comparison for a treatment at 450 °C. The sample I301/A is in fact the one of the previous treatment at 300 °C (so it had been subjected to thermal treatments at 200 and 300 °C), while the sample I301/C had not undergone any thermal treatment before the one at 450 °C. The lines indicate the concentration of  $E'_\gamma$  centres before the beginning of the thermal treatment at 450 °C in the samples I301/A (solid line) and I301/C (dashed line).

From these figures we observe that the concentration of  $E'_\gamma$  centres at the beginning of each thermal treatment is different in the two samples, due to the fact that in the pretreated samples it decreased during the preliminary thermal treatments. It can be easily observed that, notwithstanding this difference, the annealing curves of the two samples, at each temperature, tend to the same value.

A quantitative comparison between the effects of the different sequences of thermal treatments can also be made. In table 1 the variations of the concentration of  $E'_\gamma$  centre after each treatment are listed. It can be observed that the

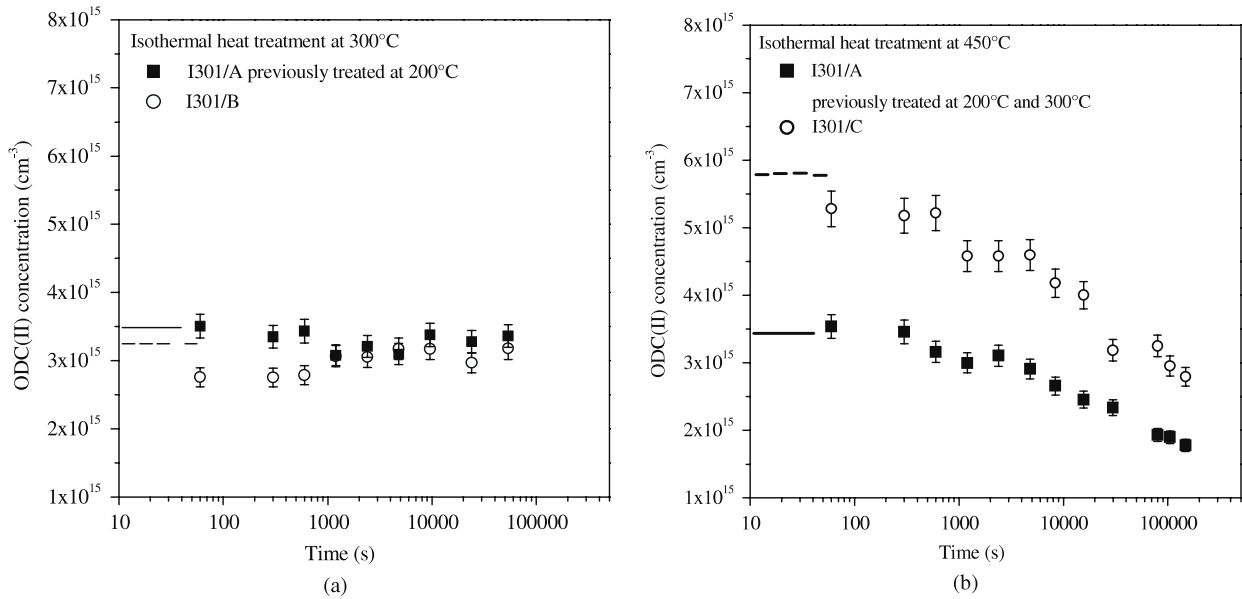


**Figure 4.** (a) Concentration of ODC(II) centres as a function of the treatment time at 300 °C, as detected in the samples I301/A, previously treated at 200 °C (filled symbols), and I301/B, not previously treated (open symbols). Solid and dashed lines represent the concentration of ODC(II) centres respectively in the samples I301/A and I301/B before the beginning of the treatment at 300 °C. (b) Concentration of ODC(II) centres as a function of the treatment time at 450 °C, as detected in the samples I301/A, previously treated at 200 °C and 300 °C (filled symbols), and I301/C, not previously treated (open symbols). Solid and dashed lines represent the concentration of ODC(II) centres respectively in the samples I301/A and I301/C before the beginning of the treatment at 450 °C.

$E'_\gamma$  concentration change following the thermal treatment at 300 °C of the sample I301/B is equal to the sum of the analogous variations observed in the sample I301/A after the treatments at 200 and 300 °C. In the same way the  $E'_\gamma$  concentration change following the thermal treatment at 450 °C of the sample I301/C is equal to the sum of the analogous variations observed in the sample I301/A after the treatments at 200, 300 and 450 °C. This result means that the total number of point defects annealed at a given temperature does not depend on the sequence of thermal treatments leading to such temperature, but only on the final temperature value. In other words the concentration of  $E'$  centres tends to a value that is function of the temperature alone, and that does not depend on the sequence of thermal treatments the sample has undergone.

Moreover, another noteworthy evidence is that the rate of the annealing process of the  $E'_\gamma$  centres is smaller in the pretreated sample at both temperatures, as can be easily observed in the figures.

The same comparison has been carried out for the ODC(II) centre, and the results are shown in figure 4. No significant change in the ODC(II) concentration is observed at 300 °C, while such concentration tends to the same value in both samples at 450 °C, as already observed for  $E'_\gamma$  centres.

So an asymptotic value for the concentration of a given defect exists, that is function of the annealing temperature alone.

### 3.2. Treatments on Silica EQ906

In this second experiment the samples Q906/A and Q906/B, whose characteristics have been described in section 2.2, have been used.

As already mentioned, the concentration of ODC(II) in the second sample is higher than in the first one, due to a higher irradiation dose. The sample Q906/B has then been subjected to a thermal treatment at 470 °C aimed at making the concentration of ODC(II) equal to the one in the Q906/A sample. At the end of this treatment the concentration of ODC(II) in the sample Q906/B is  $9 \times 10^{14}$  centres cm<sup>-3</sup>, very close to that in the Q906/A ( $1 \times 10^{15}$  centres cm<sup>-3</sup>). From this moment on the two samples have been subjected to the same isothermal treatment at 450 °C, that is a temperature lower than that of the pre-treatment of the sample Q906/B. It is worth noticing that this procedure is substantially different from that followed in the previous experiment, as in that case the pre-treatment of the samples was done at a lower temperature than that of the final annealing; a further difference with respect to the previous experiment is that in this second case the pre-treatment at 470 °C lasts the time needed to make the ODC(II) concentration in the Q906/B sample equal to the one in the Q906/A, and so the concentration at the end of this pre-treatment is not the asymptotic concentration relative to the temperature  $T = 470$  °C.

In figure 5 the isothermal anneal curves at 450 °C for (a) the ODC(II) and (b)  $E'_\gamma$  centres in the samples Q906/A and Q906/B are shown. It can be observed that the dependence of the defects concentration on time for the thermal treatment at 450 °C is rather different in the two samples; in particular the effect of the annealing process is much smaller in the sample Q906/B, that had been pretreated at 470 °C. In this sample in fact the annealing rates of both the defect studied are sensibly smaller than the analogous rates in the Q906/A sample.

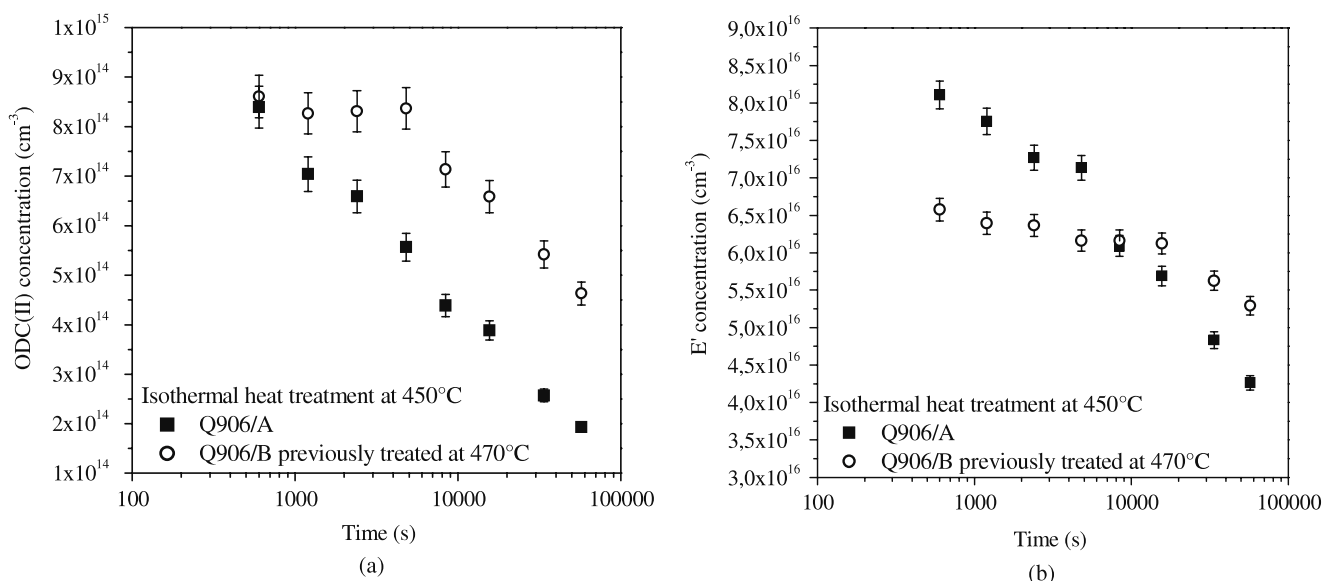


**Figure 5.** Concentration of (a) ODC(II) and (b)  $E'_\gamma$  centres as a function of the treatment time at 450 °C, as detected in the samples Q906/A (filled symbols), and Q906/B, previously treated at 470 °C (open symbols).

#### 4. Discussion

The aim of the two performed experiments was to investigate the dependence of the thermal sensitivity of oxygen deficient point defects on the thermal history of the sample, and the possible influence of the amorphous structure of the material on such property.

The possible microscopic models for these annealing processes in the temperature range from 200 °C up to 450 °C have been discussed in the introduction; diffusion–reaction mechanisms involving molecular oxygen and water have been put forward [1, 12]. From the isothermal annealing curves alone, it would not be possible to state which of these chemical species is responsible for the observed annealing of  $E'_\gamma$  and ODC(II). Notwithstanding this consideration, it had been possible to rule out a significant contribution of molecular oxygen to these processes. In fact, the  $O_2$  concentration before the thermal treatments in all the samples was lower than  $5 \times 10^{16}$  molecules  $cm^{-3}$ , that is an amount lower than the smallest  $E'_\gamma$  concentration variation observed in the samples examined (see table 1). This upper limit value of  $O_2$  has been estimated by measuring the Raman spectrum of the samples studied; in fact the PL band at 1272.2 nm (Raman shift  $\approx 1539$   $cm^{-1}$ ), observed in the Raman spectrum of samples having an oxygen concentration higher than  $5 \times 10^{16}$  molecules  $cm^{-3}$  (see section 2.1), is absent in all the samples here examined, as can be observed for the I301/A sample in figure 6.

The exclusion of oxygen leads water molecules to be the main candidate as the origin of the annealing of ODC(II) and  $E'_\gamma$  centres in the explored temperature range. Water molecules can be present in silica as the result of the process of production of the material, or can be induced during irradiation by a radiolytic process.

As reported in the first paragraph of the previous section, it has been observed that at long treatments time the

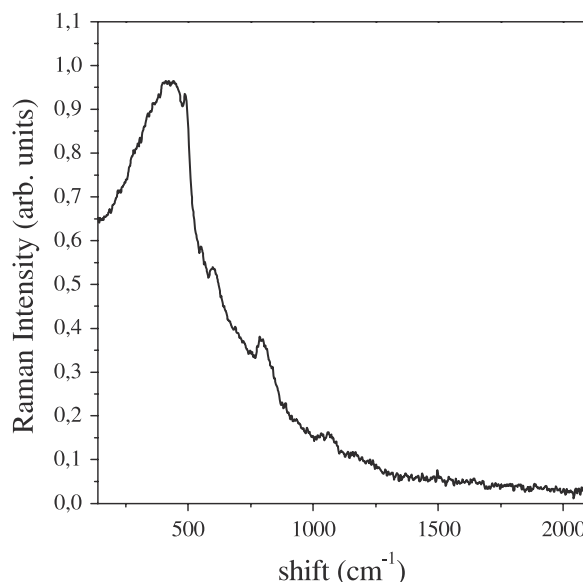


**Figure 6.** Raman spectrum of the I301/A sample. The spectrum quality is affected by fluorescence induced by the  $\beta$  irradiation. However this fact does not influence the 1540  $cm^{-1}$  region.

defect concentration has a stationary value depending on the temperature alone.

In the second paragraph of the results section, moreover, it has been observed that the annealing rate of both the defects at a given temperature  $T_1$  is much lower in a sample pretreated at a temperature  $T_2 > T_1$ , higher than the one of the treatment under examination.

Both these experimental results can be explained in the framework of the existence of a statistical distribution of the activation energy of the diffusion–reaction process. In a simple way of looking at the problem, one can imagine that each defect has its own characteristic activation energy value, which

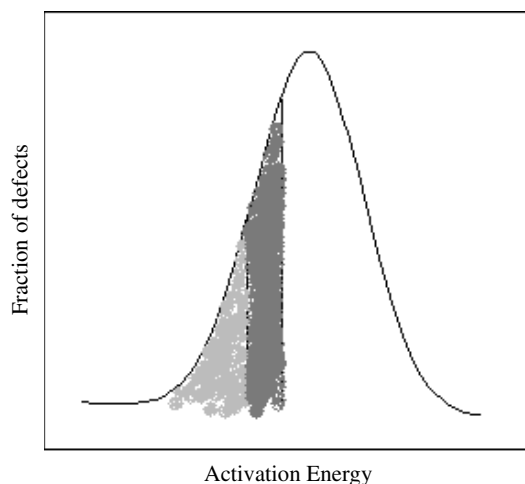


**Figure 7.** Schematic picture representing a distribution of the activation energies of the annealing process of the defects.

is statistically distributed within the population of defects. The existence of this distribution of the activation energy implies that only a certain part of the total number of defects can react at a given temperature, the ones with activation energy values equal or lower than an appropriate one. Moreover the existence of a distribution of activation energies also implies a distribution of reaction rates, as to smaller activation energies correspond higher rates.

As a consequence, in the first experiment the final concentration of defects at a given temperature after a long treatment time depends only on the temperature itself and not on previous thermal treatments at lower temperatures to which the sample has been subjected; the reason of this behaviour is that the final amount of defects annealed is the total number of defects whose annealing activation energy is low enough to let the reaction take place at the treatment temperature. This idea can be more easily understood looking at a schematic picture of the hypothesized distribution of activation energies (figure 7). The light grey part of the distribution represents the defects with activation energies such that they can react at temperatures  $T < T_1$ , while the dark grey part represents those that can react at temperatures  $T_1 < T < T_2$  ( $T_1 < T_2$ ). When a thermal treatment at the temperature  $T_2$  is performed, all the defects, the light and dark grey, are removed at the same time; when instead a sequence of two treatments at the temperatures  $T_1$  and  $T_2$  ( $T_1 < T_2$ ) is performed, during the first one the light grey defects are removed, whereas during the second one the dark grey centres are annealed. The light grey defects, having smaller activation energies than the dark grey centres, also have higher reaction rates, and this fact also explain the differences in rates observed. In conclusion, whatever the sequence of thermal treatments, at the end of the treatment at  $T_2$  both the light and dark grey defects are removed, so the total number of defects annealed depends only on the temperature  $T_2$ , as observed.

In the same way the second experiment shows that the annealing rate at a temperature  $T_1$  is much smaller in a sample pretreated at a temperature  $T_2 > T_1$ . It is possible to guess that this happens because the portion of defects able to react

at the temperature  $T_1$  has already been significantly annealed during the pre-treatment at  $T_2 > T_1$ . In other words this second experiment gives evidence that the pre-treatment has significantly changed the distribution of the activation energies of the annealing process, affecting the thermal sensitivity of the defects.

All these considerations lead to the conclusion that a statistical distribution of the activation energies of the diffusion–reaction process exists. The existence of this distribution is also the origin of the dependence of the thermal properties of point defects on the thermal history of the sample, as different histories can give rise to differences in the distributions. The existence of this distribution of activation energies can easily be physically interpreted referring to the fact that these processes take place inside an amorphous structure.

In general two distinct contributions can be associated to the observed activation energy, deriving from the diffusion phenomenon and from the reaction process, although in some cases one of them can be overriding. The former is a thermally activated process, as the motion of a molecule from one interstitial site to another one needs to overcome a potential barrier due to the geometrical arrangements of the lattice atoms; in an amorphous structure each lattice site is different, and this leads to a distribution of these potential barriers and consequently of the associated activation energy for the diffusion process.

Concerning the activation energy for reaction, we observe that it is well known that the slightly different environments surrounding the defects have influence on the optical properties of the centre itself, determining a broadening of the absorption lines due to the existence of a distribution of the transition energies [36]; in the same way as the electronic transition energies are distributed, the energies required to a reaction process to happen are distributed too, as a consequence of the differences in the defects environments. It can be concluded that, it does not matter which one is the preponderating contribution to the activation energy of the overall diffusion–reaction process, this activation energy is distributed as a consequence of the disorder characteristic of the amorphous system in which the phenomenon takes place.

Nevertheless, in the experiment shown in this paper, all the comparisons have been made between samples undergoing the same treatment at the same temperature, and differing only for their previous thermal history. Moreover no modification in the Raman spectra, and consequently in the structure of the glass matrix on which the diffusion properties of a given molecule depend, has been observed after the pretreatments of the samples. As a consequence it can be stated that the diffusion properties are the same in the couples of samples compared, and the differences observed are due to differences in the activation energy distribution for the reaction process, that therefore is the limiting one here. The fact that the key step in the diffusion–reaction process that causes the annealing of oxygen deficient point defects is the reaction also explains differences in the behaviour of different centres reacting with the same molecule at the same temperature, as to different defects corresponds different activation energies of the reaction with the same species.



## 5. Conclusions

We have reported experimental results on the effects of sequences of isothermal treatments on two irradiation induced defects in silica, the ODC(II) and the  $E'_{\gamma}$  centre. In particular we have investigated the influence that the amorphous structure of the matrix has on the thermal properties of the defects. The results reported here give direct evidence that a statistical distribution of the activation energies of the reaction process exists, and that it gives rise to a dependence of the thermal sensitivity of point defects on the thermal history of the sample, as different histories can give rise to differences in the distributions. The existence of such a distribution of activation energies is intimately related to the intrinsic disorder of the amorphous lattice, and so it can be thought to be a general feature of point defects in disordered solids.

## Acknowledgments

We thank G Buscarino, F Messina and the other people of the LAMP laboratory of Palermo for useful discussions and comments. We acknowledge R M Montereali, G Messina (ENEA, Italy) for  $\beta$  irradiation and B Brichard (SCK-CEN, Belgium) for  $\gamma$  irradiation. Partial financial support by POR Sicilia 2000/2006 Misura 3.15–Sottoazione C and technical assistance by G Napoli and G Tricomi are gratefully acknowledged.

## References

- [1] Griscom D L 1986 *Structure and Bonding in Noncrystalline Solids* ed G E Walrafen and A G Revesz (New York: Plenum) pp 369–83
- [2] Pacchioni G, Skuja L and Griscom D L (ed) 2000 *Defects in SiO<sub>2</sub> and Related Dielectrics: Science and Technology* (Dordrecht: Kluwer–Academic) ISBN 0-7923-6685-9
- [3] Bakos T, Rashkeev S N and Pantelides S T 2004 *Phys. Rev. B* **69** 195206
- [4] Agnello S and Nuccio L 2006 *Phys. Rev. B* **73** 115203
- [5] Zhang L, Mashkov V A and Leisure R G 1996 *Phys. Rev. B* **53** 7182
- [6] Griscom D L 1984 *J. Non-Cryst. Solids* **68** 301
- [7] Griscom D L 1985 *J. Non-Cryst. Solids* **73** 71
- [8] Kajihara K, Skuja L, Hirano M and Hosono H 2004 *Phys. Rev. Lett.* **92** 015504
- [9] Skuja L 2005 *Phys. Status Solidi c* **2** 15
- [10] Skuja L 1998 *J. Non-Cryst. Solids* **239** 16
- [11] Imai H, Arai K, Imagawa H, Hosono H and Abe Y 1988 *Phys. Rev. B* **38** R12772
- [12] Griscom D L 1984 *Nucl. Instrum. Methods Phys. Res. B* **1** 481
- [13] Arai K, Imai H, Hosono H, Abe Y, Imagawa H and Hosono H 1988 *Appl. Phys. Lett.* **53** 1891
- [14] Zatsepin A, Kortov V S and Fitting H-J 2005 *J. Non-Cryst. Solids* **351** 869
- [15] Skuja L, Streletsky A N and Pakovich A B 1984 *Solid State Commun.* **50** 1069
- [16] Pacchioni G and Ferrario R 1998 *Phys. Rev. B* **58** 6090
- [17] Nuccio L, Agnello S, Boscaino R, Boizot B and Parlato A 2007 *J. Non-Cryst. Solids* **353** 581
- [18] Messina F and Cannas M 2007 *J. Phys. Chem. C* **111** 6663
- [19] Li Z, Fonash S J, Poindexter E H, Harmatz M, Rong F and Buchwald W R 1990 *J. Non-Cryst. Solids* **126** 173
- [20] Smith C M, Borrelli N F and Araujo R 2000 *J. Appl. Opt.* **39** 5778
- [21] Griscom D 1985 *J. Appl. Phys.* **58** 2524
- [22] Kajihara K, Skuja L, Hirano M and Hosono H 2006 *Phys. Rev. B* **74** 094202
- [23] Messina F and Cannas M 2005 *Phys. Rev. B* **72** 195212
- [24] Kajihara K, Skuja L, Hirano M and Hosono H 2002 *Phys. Rev. Lett.* **89** 135507
- [25] Edwards A H and Fowler W B 1982 *Phys. Rev. B* **26** 6649
- [26] Radtsig V A 1998 *J. Non-Cryst. Solids* **239** 49
- [27] Radtsig V A, Baskir E G and Korolev V A 1995 *Kinet. Catal.* **36** 568
- [28] Radtsig V A, Baskir E G and Korolev V A 1995 *Kinet. Catal.* **36** 142
- [29] Kajihara K, Miura T, Kamioka H, Hirano M, Skuja L and Hosono H 2004 *J. Non-Cryst. Solids* **349** 205
- [30] Agnello S, Boscaino R, Cannas M and Gelardi F M 2001 *Phys. Rev. B* **64** 174423
- [31] Skuja L, Güttler B, Schiel D and Silin A R 1998 *J. Appl. Phys.* **83** 6106
- [32] Hetherington G, Jack K H and Ramsey M W 1965 *Phys. Chem. Glasses* **6** 6
- [33] *Catalogue POL-0/102/E* (Hanau: Heraeus Quartzglas)
- [34] *Catalogue OPT-91-3* (Nemours: Quartz and silice)
- [35] Agnello S, Boscaino R, Buscarino G, Cannas M and Gelardi F M 2002 *Phys. Rev. B* **66** 113201
- [36] Nalwa H S (ed) 2001 *Silicon-Based Materials and Devices* (New York: Academic) ISBN 0-12-513909-8